

Towards Analyzing the Effect of Interference Monitoring in GNSS Scintillation

*Original*

Towards Analyzing the Effect of Interference Monitoring in GNSS Scintillation / ROMERO GAVIRIA, RODRIGO MANUEL; DAVIS, Fabio - In: Mitigation of Ionospheric Threats to GNSS: an Appraisal of the Scientific and Technological Outputs of the TRANSMIT Project / Notarpietro R, Davis F., De Franceschi G. Aquino M.. - ELETTRONICO. - Reijka, Croatia : InTech, 2014. - ISBN 9789535116424. - pp. 37-48 [10.5772/58768]

*Availability:*

This version is available at: 11583/2555545 since:

*Publisher:*

InTech

*Published*

DOI:10.5772/58768

*Terms of use:*

This article is made available under terms and conditions as specified in the corresponding bibliographic description in the repository

*Publisher copyright*

(Article begins on next page)

---

# Towards Analyzing the Effect of Interference Monitoring in GNSS Scintillation

---

Rodrigo Romero and Fabio Dovis

Additional information is available at the end of the chapter

<http://dx.doi.org/10.5772/58768>

---

## 1. Introduction

Electron concentration in the ionosphere affects GNSS (Global Navigation Satellite Systems) signals by introducing delays in their propagation. Such error can be corrected in part by making use of models of the background ionosphere when performing single frequency measurements, or entirely in the case of dual frequency measurements. In some cases electron density irregularities may appear that can disrupt further the propagation of the wave introducing fluctuations in amplitude and phase called scintillations [1].

How often GNSS signals are affected by scintillations depends on solar and geomagnetic activity, geographic location, season, local time and signal frequency. Amplitude scintillations cause signals to fade. Phase scintillations may induce a frequency shift in the signal carrier that in some cases can go beyond the Phase Lock Loop (PLL) bandwidth of the GNSS receiver. Both effects are very challenging for a receiver and may cause frequent cycle slips and losses of lock of the satellite signals during strong ionospheric events [2].

Ionospheric Scintillation Monitoring Receivers (ISMR) are specialized GNSS receivers able to track and monitor scintillations in order to collect data that can be used to model the phenomenon, study its affects at receiver level and possibly predict its occurrence in the future. Such receivers are able to measure the amount of scintillation affecting a satellite signal in both amplitude and phase by making use of correlation data from the tracking processing blocks. This is normally done by computing two indices: the S4 for amplitude scintillation and the phase deviation due to scintillations [3].

However, as more telecommunication systems are likely to work in frequency bands close to GNSS signals in the next years, monitoring of scintillation activity might be threatened by the presence of Radio Frequency Interference (RFI) in the operation area. It is of interest to study the effects these systems may have on the estimation of scintillation indices due to uninten-

tional leakages of power out of their allocated bandwidth [4]. Robust tracking of GNSS signals under such conditions must be guaranteed and it must also be ensured as best as possible that the typical scintillation indices are not affected by the additional error source.

In this paper we deal with a specific environment of an ISMR where the monitoring of scintillation activity is threatened by the presence of interference. Section II offers some background on ionospheric scintillation measurements with GNSS receivers. Section III describes the interference scenarios. Section IV describes the set-up of a monitoring station deployed and installed in the city of Hanoi in Vietnam to collect real scintillating signals samples. Section V presents the results. Finally, conclusion and future work to be developed are summarized in Section VI.

## 2. Ionospheric scintillation measurements with GNSS receivers

The mathematical expression of the current GPS L1 C/A signal affected by scintillation can be written as:

$$S(t) = A\delta A(t)d_{L_1}(t)c_{L_1}(t)\sin(2\pi f_{L_1}t + \varphi + \delta\varphi(t)) \quad (1)$$

Where  $A$  is the signal amplitude,  $\delta A(t)$  is the amplitude fluctuation due to scintillation,  $d(t)$  is the navigation data with a rate of 50Hz,  $c(t)$  is the PRN spreading code with period of 1ms,  $f_{L_1}$  is the radiofrequency carrier,  $\varphi$  is the initial carrier phase and  $\delta\varphi(t)$  is the phase fluctuation due to scintillation. Scintillation is measured by 2 indices: S4 for amplitude scintillation and  $\sigma\varphi$  (phase deviation) for phase scintillation. These are usually computed over an observation interval  $T_{obs}=60s$ , as described in [3].

The S4 index is the standard deviation of the Signal Intensity (SI) normalized by its mean value. It is calculated from the in-phase and quadrature-phase accumulation samples of the prompt correlator. The total S4 is calculated as:

$$S4_T = \sqrt{\frac{\langle SI^2 \rangle - \langle SI \rangle^2}{\langle SI \rangle^2}} \quad (2)$$

Where  $\langle \rangle$  represents the expected (or average) value over  $T_{obs}$ . If the carrier to noise density  $C/N_0$  can be estimated during  $T_{obs}$  it is possible to have an estimate of the S4 due to noise:

$$S4_n = \sqrt{\frac{100}{C/N_0} \left( 1 + \frac{500}{19^2 C/N_0} \right)} \quad (3)$$

The revised S4 without the noise contribution is obtained as:

$$S4 = \sqrt{S4_T^2 - S4_n^2} \quad (4)$$

The phase standard deviation index  $\sigma\phi$  is calculated as the standard deviation of the phase fluctuations due to scintillations,  $\delta\phi(t)$  in (1). Such fluctuations correspond to the high-frequency portions of the carrier phase. Though it cannot be measured directly by the receiver,  $\delta\phi(t)$  can be estimated by detrending the carrier phase measurements from the satellite signals. The method widely used for detrending is to pass raw 50Hz phase measurements through a sixth order high pass Butterworth digital filter with cut-off frequency of 0.1Hz.

### 3. Interference scenarios

Radio frequency interference is, among the different error sources that corrupt satellite navigation waveforms, a particularly harmful error since in some cases it cannot be mitigated by a simple correlation process. This is indeed a problem that may affect the detection of ionospheric scintillation when monitored by GNSS signals, and will be analyzed in several interference scenarios. The scintillating signal affect by interference is given by

$$S\_interf(t) = S(t) + i(t) \tag{5}$$

Where  $S(t)$  is a GNSS scintillating signal as defined in (1) and  $i(t)$  is the interference signal and can assume different forms depending on the system that generated it. Two types of interferences were generated and fed into the receiver along with the scintillating signal: A narrowband interference in the form of a Continuous Wave (CW) and a wideband interference in the form of a Chirp Signal (CS). Figure 1 shows the spectrum of an unperturbed GNSS signal along with the interfered versions.

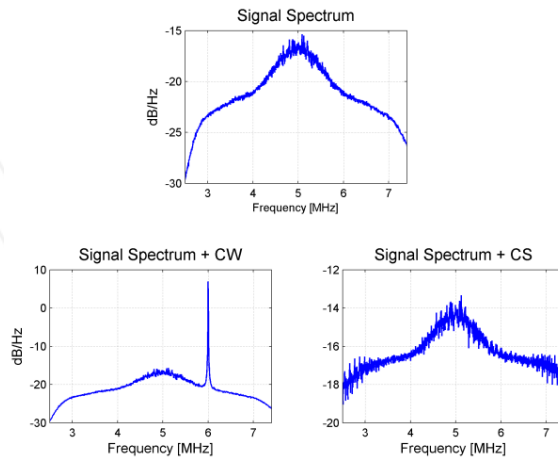
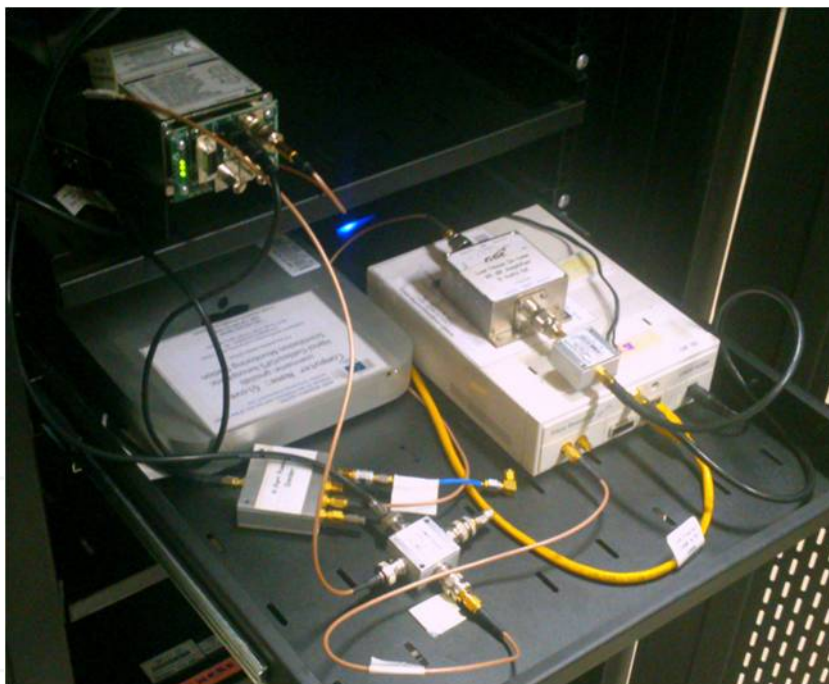


Figure 1. Spectra of Clean and Interfered Signals.

#### 4. Scintillation data collection at Hanoi

A GNSS front-end based on a general purpose Universal Software Radio Peripheral (USRP) was installed in Hanoi, Vietnam ( $21^{\circ} 2' 0''$  N /  $105^{\circ} 51' 0''$  E) for ionospheric scintillation data collection. The set up took place at the NAVIS Centre, Hanoi University of Science and Technology in collaboration with the European Joint Research Center based in Ispra, Italy and the NavSaS group of Politecnico di Torino / Istituto Superiore Mario Boella based in Turin, Italy. The installation consisted of an antenna AT1675-120W SEPCHOKE\_MC with Spike Radome, an Ettus Research USRP Model N200 front-end with baseband low pass filter of 2MHz cut-off frequency, coupled with a 10MHz Rubidium reference oscillator, pc and hard drives as seen in Figure 2. Data were collected from February to September 2013 at 5MSamples/sec in the L1/E1 band in a 20 minutes basis each day after sunset local time. A fully software receiver as presented in [5] and updated to process scintillating GPS signals was used to post-process the data coming from the USRP and calculate the scintillation indices.



**Figure 2.** Hardware installed at Hanoi for collection of GNSS scintillating signals.

In parallel to the USRP data collections, a Septentrio PolaRx4 receiver was set up to continuously log regular observables such as C/N0, azimuth and elevation of available satellites from both GPS and Galileo. Through a replay process of the USRP logged data, scintillation indices are obtained from a Septentrio PolaRxS [6] for comparison purposes.

#### 4.1. Scintillation observations

Figure 3 shows  $C/N_0$  and correlator outputs for a GPS scintillating satellite, PRN23, acquired from a dataset during the 14 of March 2013, 1440UTC. As can be seen from the top plot, the so called focusing-defocusing effect of scintillation in the signal amplitude causes the power in the prompt correlator to fluctuate. The effect is also noticeable in the estimated  $C/N_0$ .

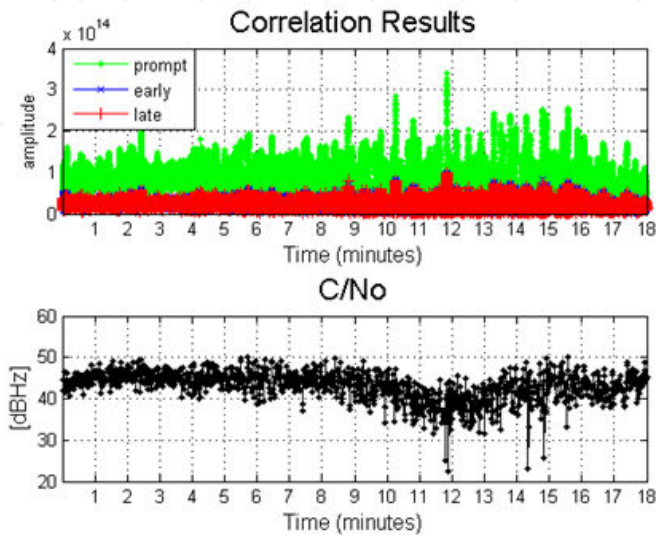


**Figure 3.** Correlation results (top) and estimated  $C/N_0$  (bottom) for GPS PRN23.

Figure 4 shows the estimated scintillation indices  $S_4$  and  $\sigma_\phi$  (60s version) from the software receiver against the indices calculated by Septentrio's PolaRxS. For the software receiver, the tracking architecture consisted of a third order PLL with 12Hz bandwidth and integration time of 1ms. As can be seen there is a good agreement between the software receiver calculated indices with those from the PolaRxS, the latter used as a benchmark for our results. It is observed from the top plot of Figure 4 that the satellite was quite affected by scintillation, going from medium to very strong amplitude scintillation levels in the 18 minutes of processed data. To recall,  $S_4$  above 0.6 is considered strong in the literature.

The bottom plot of Figure 4 corresponds to the phase scintillation index  $\sigma_\phi$ . There is no value shown for the index during the first four minutes of data processing due to the transient time of the detrending filter of the phase measurements. Severe scintillation activity may lead  $\sigma_\phi$  in particular not being calculated at all if the satellite losses lock continuously.

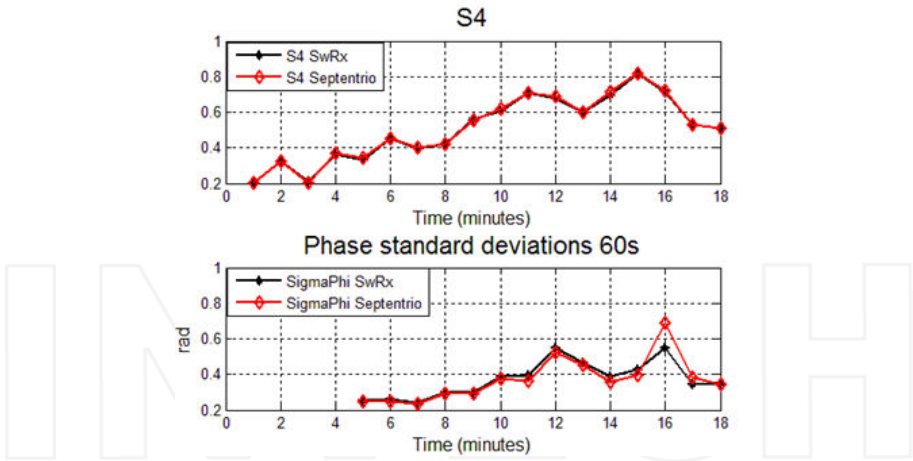


Figure 4. Software receiver computed S4 (top) and  $\sigma_\phi$  (bottom) vs Septentrio PolaRxS for GPS PRN23

## 5. Results

The same dataset was contaminated by interference in order to observe its effect on the scintillation indices measurements. The operation was performed from minutes 5 to 14, as can be seen in Figure 5 for the comparison of the estimated C/N0 of one of PRN13 before and after the CW interference was injected. As observed in the figure, under interference GNSS receivers experience a drop in signal power and an increased variance in the signal amplitude.

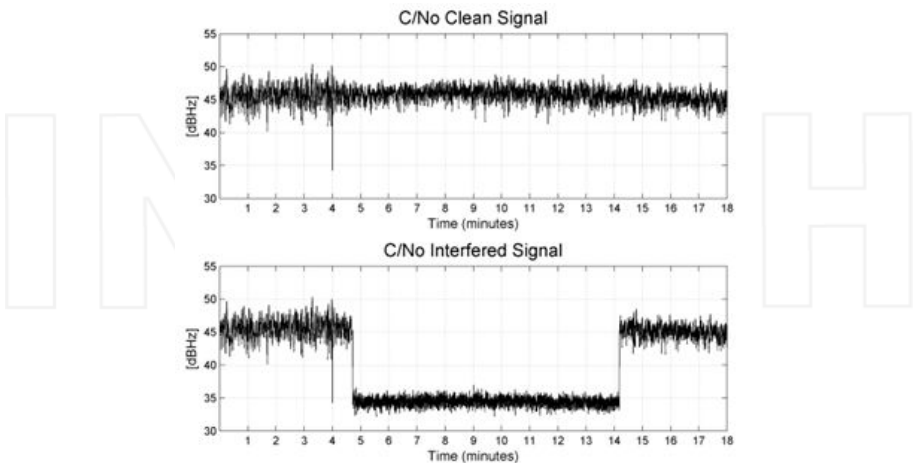


Figure 5. PRN11 C/N0 nominal case (top) vs. interfered case (bottom).

Figures 6 and 7 show the scintillation indices calculated under the effect of the CW and CS interferences for PRN11. As observed, the S4 index showed variations due to the interference, whereas the phase index remained largely unchanged. Given that the S4 index is calculated over the fluctuations of the signal intensity, it is indeed more vulnerable to additional error sources that also cause the signal power to fluctuate. However, how much the index will be affected if at all might ultimately depend on the relative power of the interference with respect to the signal, for how long it is active and the type of interference.

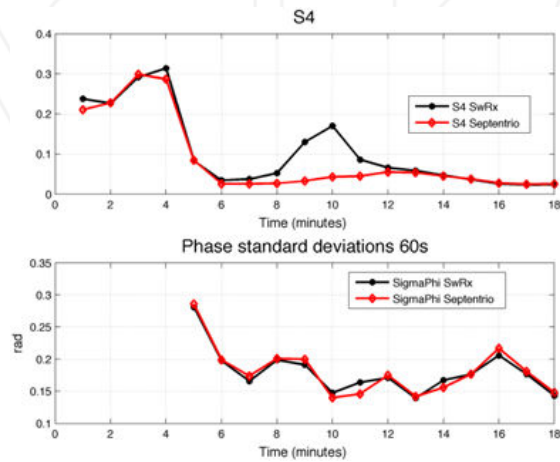


Figure 6. PRN11 S4 (top) and  $\sigma\phi$  (bottom) under CW interference.

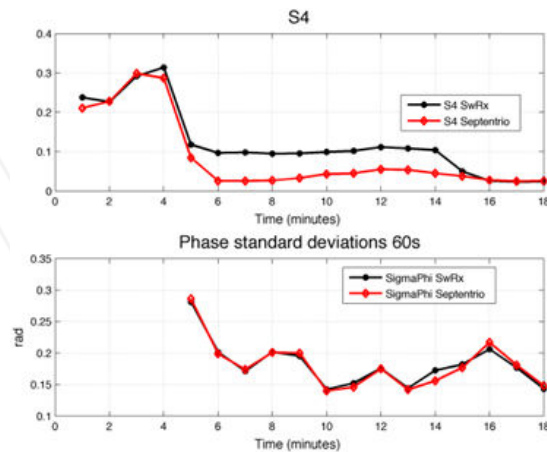


Figure 7. PRN11 S4 (top) and  $\sigma\phi$  (bottom) under CS interference.



To demonstrate, Figures 8 and 9 show the indices calculated for a different satellite, PRN13, in the same scenarios as before. It can be seen that indices for PRN13 barely changed. This is understandable as PRN13 presents a stronger level of scintillations than PRN11, so fluctuations introduced by the interference signals don't stand out as much as before.

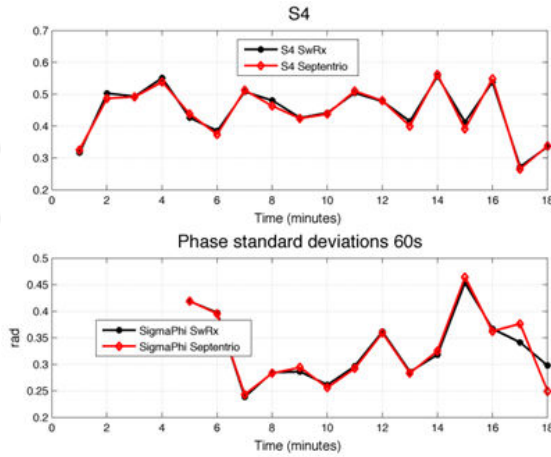


Figure 8. PRN13 S4 (top) and  $\sigma\phi$  (bottom) under CW interference.

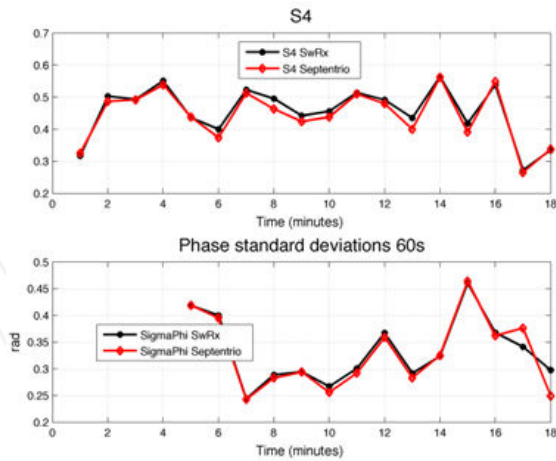
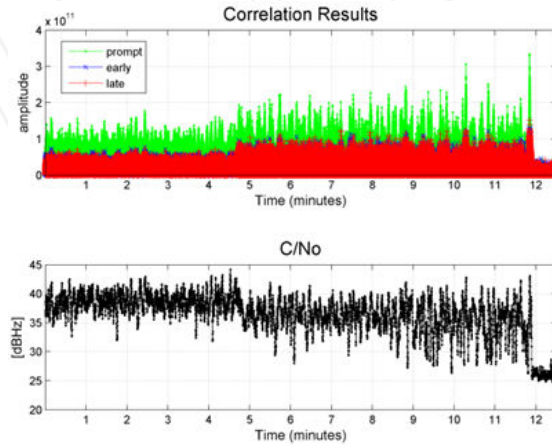


Figure 9. PRN13 S4 (top) and  $\sigma\phi$  (bottom) under CS interference.

In some cases, however, even if the effect of interference is not entirely reflected over the indices the combined effect of scintillation plus interference may prove too difficult for the receiver to

track. This ultimately leads to a loss of lock of the satellite signal and a wrong estimation of the ionospheric scintillation, as shown in Figures 10 and 11 for PRN23, a satellite with strong scintillation. Compared to the previous case in Figures 4 and 5 where PRN23 was successfully tracked in its scintillation only scenario, it is noticeable now that at the point when scintillations are very high the receiver is not able to cope with both the scintillations and the added fluctuations introduced by the interference signal.



**Figure 10.** Correlation results (top) and estimated C/N0 (bottom) for GPS PRN23 under CW interference.

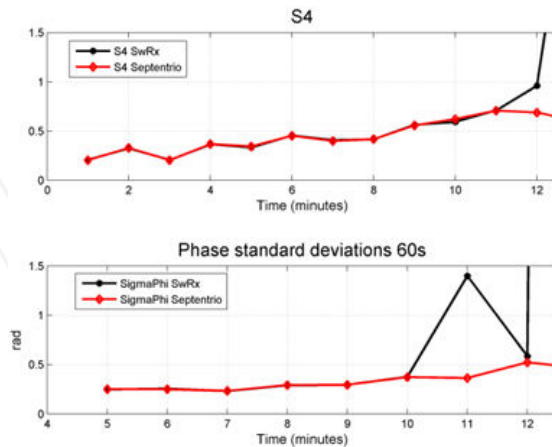


**Figure 11.** Software receiver computed S4 (top) and  $\sigma_\phi$  (bottom) vs Septentrio PolaRxS for GPS PRN23 under CW interference.

## 6. Conclusion

A preliminary analysis of the effect of interference signals in the monitoring of ionospheric scintillation events was presented. Out of the two most common scintillation measurements with GNSS, the amplitude scintillation index S4 seems to be more susceptible to suffer variations due to the presence of external signals as compared to the phase deviation index. It was also shown that the combined effects of both scintillation and interference stresses the tracking blocks within the receiver to the point where losses of lock of the signals become more frequent. Nevertheless, the impact might ultimately depend on the level of scintillation of a given PRN and several characteristics of the interference itself: power, bandwidth and duration. Future work will continue to address the effect of interference on scintillation monitoring while taking into account the possibility to detect and mitigate the interference itself.

## Acknowledgements

This research work is undertaken under the framework of the TRANSMIT ITN funded by the Research Executive Agency within the 7th Framework Program of the European Commission, People Program, Initial Training Network, Marie Curie Actions.

## Author details

Rodrigo Romero\* and Fabio Dovis

\*Address all correspondence to: rodrigo.romero@polito.it

Department of Electronics and Telecommunications, Politecnico di Torino, Italy

## References

- [1] K. C. Yeh and C.-H. Liu. Radio wave scintillations in the ionosphere. In Proceedings of the IEEE, vol. 70, no. 4, 1982, pp. 324–360J.
- [2] P. H. Doherty, S. Delay, C. Valladares, and J. Klobuchar. Ionospheric Scintillation Effects in the Equatorial and Auroral Regions. In Proceedings of the 13th International Technical Meeting of the Satellite Division of the Institute of Navigation (ION GPS 2000). Salt Lake City, UT. pp. 662–671.

- [3] A. V. Dierendonck and Q. Klobuchar, "Ionospheric Scintillation Monitoring Using Commercial Single Frequency C/A Code Receivers," in Proc. ION GPS, 1993, pp. 1333–1342.
- [4] B. Motella, M. Pini, and F. Dovis, "Investigation on the effect of strong out-of-band signals on global navigation satellite systems receivers," GPS Solutions, vol. 12, pp. 77–86, 2008. M. Young, The Technical Writer's Handbook. Mill Valley, CA: University Science, 1989.
- [5] K. Borre. Software-defined GPS and Galileo receiver: A single-frequency approach. Boston: Birkhauser. 2007.
- [6] B. Bougard, J. Sleewaegen, L. Spogli, S. Veetil, S. & J. Galera. CIGALA: Challenging the Solar Maximum in Brazil with PolaRxS. In Proceedings of the 24th International Technical Meeting of The Satellite Division of the Institute of Navigation (ION GNSS 2011). Portland, OR, USA. 2011. pp. 2572-2579.

INTECH

